CYLINDRICAL PISTON PROBLEM IN WATER

I. *Artificial Viscosity Method*

B. C. PANDEY & PHOOLAN PRASAD

Indian Institute of Science, Bangalore

(*Received* 1 *November*, 1968 ; *revised* 15 *March*, 1969)

A study of compression waves produced in water by the non-uniform expansion of a cylindrical piston of non-zero initial radius is made by the artificial viscosity method of von Neumann & Richtmyer. It is found that the damping effect introduced by the cylindrical geometry is much less pronounced than that of the spherical geometry.

In the present paper, we have studied compression waves produced in water by the expansion of a cylindrical piston. If the piston expands with uniform speed and its initial radius is zero, then the motion is self-similar and the solution of this problem can be easily found out by the numerical integration of ordinary differential equations following Taylor[1]. Lighthill[2] has discussed this problem for small mach number of the piston and has deduced that the strength of the shock, which forms the wave front, is of the order of the fourth power of the piston mach number. When the expansion of the piston is not uniform or the initial radius of the piston is non-zero, the fluid motion is not self-similar and in this case we can solve the problem only by the numerical integration of partial differential equations. Since we wish to take non-uniform expansion speed and non-zero initial radius of the piston, we have utilised the well-known artificial viscosity method of von Neumann & Richtmyer[3]. It has been shown in reference (5 referred to as paper 1 in the sequel), that artificial viscosity term of von Neumann & Richtmyer[3] can be used even if the medium is water though the thickness of the transition region depends on shock strength. In paper 1, the corresponding spherical piston problem has been discussed in detail.

EQUATION OF MOTION

We have used here the notations of von Neumann & Richtmyer[3] with the difference that X and x represent Eulerian and Lagrangian distances respectively from the axis of the cylinder. We assume the path of the piston to be given by the hyperbola

$$X = X_0' + \frac{m_1}{m} \left\{ (1 + m^2 t^2)^{\frac{1}{2}} - 1 \right\} \tag{1}$$

where m_1 represents the final asymptotic speed of the piston, $1/\sqrt{3}m$ is the time required by the piston to attain half of the final asymptotic speed and X_0' is the initial radius of the piston.

The equations governing the flow with cylindrical symmetry in Lagrangian coordinates are

$$\rho_0 \frac{\partial U}{\partial t} = - \left(\frac{X}{x} \right) \frac{\partial}{\partial x} \left(p + q \right) \tag{2}$$

$$\frac{\partial X}{\partial t} = U (x, t) \tag{3}$$

$$\frac{\partial V}{\partial t} = \frac{1}{\rho_0}\left(\frac{X}{x}\right)\frac{\partial U}{\partial x} + \frac{UV}{X} \tag{4}$$

with the equation of state[4]

$$p = \frac{A'}{V^{\gamma}} - B \tag{5}$$

$\gamma = 7$ for water and with the artificial viscosity term

$$q = -\frac{(c\triangle x)^2 \dfrac{\partial U}{\partial x}\left(\left|\dfrac{\partial U}{\partial x}\right| - \dfrac{\partial U}{\partial x}\right)}{2V} \tag{6}$$

We non-dimensionalise the set of equations (2) to (6) with the help of the undisturbed state values p_0, ρ_0, a_0 of pressure, density, sound speed and a characteristic length equal to the distance travelled by the sound wave in unit time and write the corresponding system of difference equations.

$$\frac{\overset{n+\frac{1}{2}}{U_l} - \overset{n-\frac{1}{2}}{U_l}}{\triangle t} = -\frac{1}{\gamma(1+\overline{B})}\left(\frac{\overset{n}{X_l}}{\overline{X}_0' + l\triangle x}\right) \times \frac{\overset{n}{p}_{l+\frac{1}{2}} - \overset{n}{p}_{l-\frac{1}{2}} + \overset{n-\frac{1}{2}}{q}_{l+\frac{1}{2}} - \overset{n-\frac{1}{2}}{q}_{l-\frac{1}{2}}}{\triangle x} \tag{7}$$

$$\frac{\overset{n+\frac{1}{2}}{X_l} - \overset{n}{X_l}}{\triangle t} = \overset{n+\frac{1}{2}}{U_l} \tag{8}$$

$$\frac{\overset{n+1}{V}_{l+\frac{1}{2}} - \overset{n}{V}_{l+\frac{1}{2}}}{\triangle t} = \frac{\overset{n+1}{X}_{l+1} + \overset{n}{X}_{l+1} + \overset{n+1}{X_l} + \overset{n}{X_l}}{4\left\{\overline{X}_0' + (l+\frac{1}{2})\triangle x\right\}} \cdot \frac{\overset{n+\frac{1}{2}}{U}_{l+1} - \overset{n+\frac{1}{2}}{U_l}}{\triangle x} + \frac{\left(\overset{n+\frac{1}{2}}{U}_{l+1} + \overset{n+\frac{1}{2}}{U_l}\right)\left(\overset{n+1}{V}_{l+\frac{1}{2}} + \overset{n}{V}_{l+\frac{1}{2}}\right)}{\overset{n+1}{X}_{l+1} + \overset{n}{X}_{l+1} + \overset{n+1}{X_l} + \overset{n}{X_l}} \tag{9}$$

$$\overset{n+\frac{1}{2}}{q}_{l+\frac{1}{2}} = -\frac{c^2\gamma(1+\overline{B})}{\overset{n}{V}_{l+\frac{1}{2}} + \overset{n+1}{V}_{l+\frac{1}{2}}}\left(\overset{n+\frac{1}{2}}{U}_{l+1} - \overset{n+\frac{1}{2}}{U_l}\right)\left\{\left|\overset{n+\frac{1}{2}}{U}_{l+1} - \overset{n+\frac{1}{2}}{U_l}\right| - \left(\overset{n+\frac{1}{2}}{U}_{l+1} - \overset{n+\frac{1}{2}}{U_l}\right)\right\} \tag{10}$$

$$\overset{n+1}{p}_{l+\frac{1}{2}} = \frac{\overline{A'}}{\left(\overset{n+1}{V}_{l+\frac{1}{2}}\right)^{\gamma}} - \overline{B} \tag{11}$$

From (1) we obtain the non-dimensional velocity of the position

$$Up = \frac{\overline{m}_1 \, \overline{m} \, t}{(1 + \overline{m}^2 t^2)^{\frac{1}{2}}} \tag{12}$$

The initial and boundary conditions are

$$U_l^{-\frac{1}{2}} = 0, \; q_{l+\frac{1}{2}}^{-\frac{1}{2}} = 0, \; X_l^0 = \overline{X}'_0 + l\triangle x, \; p_{l+\frac{1}{2}}^0 = 1, \; V_{l+\frac{1}{2}}^0 = 1 \tag{13}$$

for $l = 0, 1, 2. \ldots\ldots$

and

$$\left.\begin{aligned} X_0^n &= \overline{X}_0' + \frac{\overline{m}_1}{\overline{m}}\left[\left\{1 + \overline{m}^2 (n\triangle t)^2\right\}^{\frac{1}{2}} - 1\right] \\ U_0^{n+\frac{1}{2}} &= \frac{\overline{m}_1 \, \overline{m} \, (n + \frac{1}{2}) \triangle t}{[1 + \overline{m}^2 \{(n + \frac{1}{2}) \triangle t\}^2]^{\frac{1}{2}}} \end{aligned}\right\} \tag{14}$$

for $n \geqslant 1$

In (7) to (14), the bar used for non-dimensional variables has been dropped from the flow variables, but the non-dimensional parameters carry the bars.

DISCUSSION AND RESULTS

We have carried out the computations with the following values of the constants and mesh size :

$$c = 2, \gamma = 7, \overline{B} = 3000, \overline{A}' = 3001, \triangle x = 0 \cdot 00001.$$

Piston	Case	$\overline{X}_0'$	$\overline{m}_1$	$\overline{m}$	$\frac{\triangle t}{\triangle x}$	Total time up to which result is obtained
Cylindrical Piston	1.	0·0001	0·28601	10000	0·4	·0006
,,	2.	0·0001	0·97212	30000	0·1	·00028
*Spherical Piston[5]	3.	0·0001	0·97212	·30000	0·15	·00011
,,	4.	0·001	0·97212	15000	0·15	·0002

*These results have been taken from paper 1 for comparison (see reference 5).

Figs. 1, 2 and 3 show the distribution of velocity, pressure, specific volume and Eulerian distance versus Lagrangian distrance at different cycles of time. In Fig. 1, we observe that the velocity at a fixed time is greatest at the piston and it decreases as we move towards the shock front and ultimately it falls down to its zero value ahead of the shock. The velocity at the piston increases with increasing number of time cycles and it tends to its asymptotic value m_1 ultimately. It is worthy of notice that only in case 1 velocity-Lagrangian distance curves (for a fixed time) are convex with respect to x axis after a certain time. This feature is nowhere present in the spherical case discussed in earlier paper. We remark

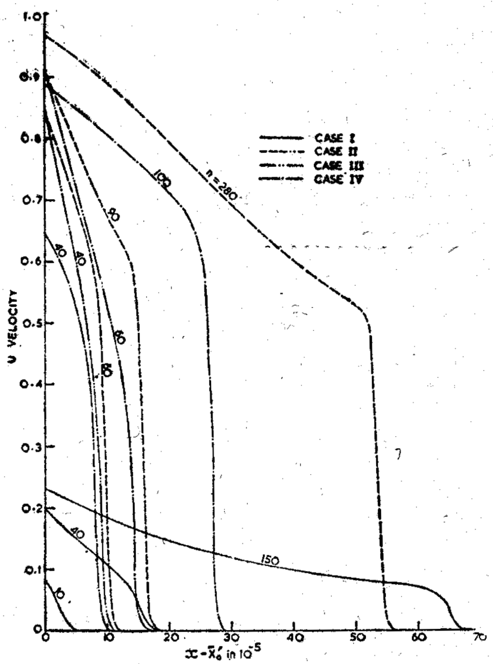

Fig. 1.—Velocity *versus* Lagrangian distance for various cycles of time.

here that after a very long time, when the shock has travelled through a distance large compared to the initial radius 'the flow tends to become self-similar'. The shock strength in case 1 is very small compared to other cases due to low piston velocity $\overline{m}_1$.

In Fig. 2, we observe that the pressure at a fixed time is greatest at the piston and it gradually decreases as we move towards the shock front and ultimately it falls down to its value 1 of the undisturbed state. The choice of our scale for pressure gives an illusion that the pressure curves end on $p = 0$; in fact they end on the line $p = 1$. Further we find that the pressure at the piston increases up to a certain time and thereafter it shows a decrease with time. It is also evident from Fig. 2 that pressure gradient throughout the wave region decreases with the increase of time and in case 1, the pressure curve is almost a straight line at $n = 150$.

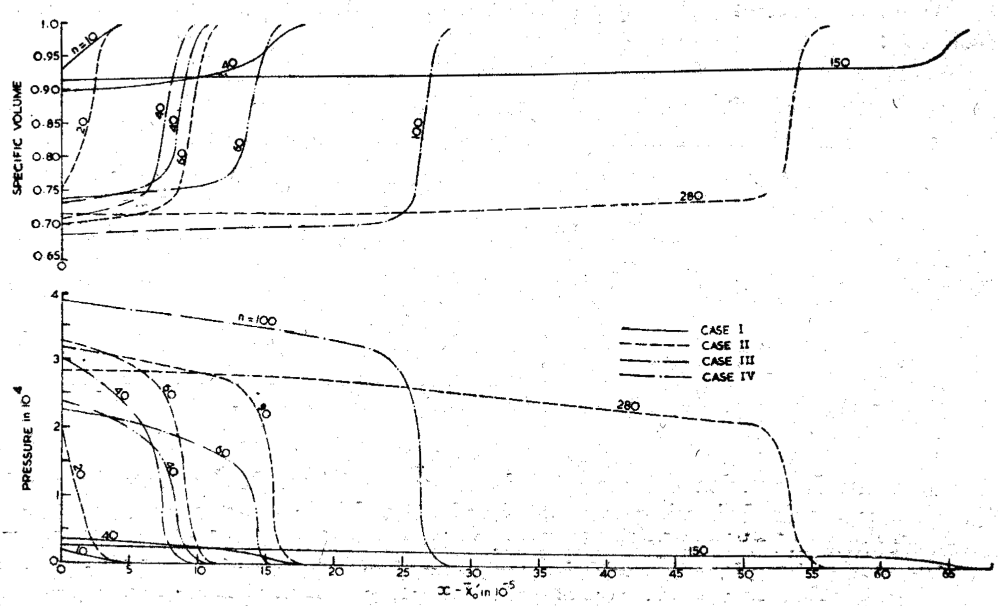

Fig. 2—(*a*) Specific Volume *versus* Lagrangian distance at various cycles of time.

(*b*) Pressure *versus* Lagrangian distance at various cycles of time.

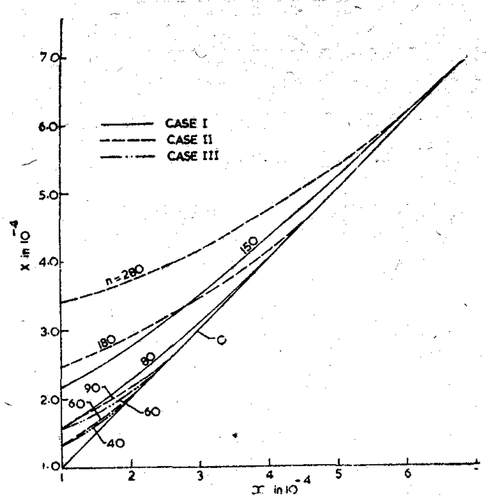

Fig. 3—Eulerian distance *versus* Lagrangian distance at various cycles of time.

Cases 2 and 3 bring out the difference in the flow pattern due to cylindrical and spherical geometry since $\overline{X}'_0$, $\overline{m}_1$, $\overline{m}$ are same in the both cases. Comparing the curves of case 3 at the cycle 40 with that at cyle 60 of case 2 (cylindrical piston), we find that the velocity distribution given by the spherical motion behind the shock at each point except at the piston is less than that given by the cylindrical motion and similarly the pressure in case 3 is everywhere small compared to that in case 2 (even at the piston), though both pistons have started with same initial radii and have moved for the same time with same acceleration. This brings out the fact that the damping effect of sphericity is stronger than that of the cylindrical geometry.

The upper part of Fig. 2 shows the distribution of the specific volume at various cycles and supports the above observations regarding pressure distribution as expected from the equation 5.

In cases 1, 2, 3 and 4 the shock has travelled about 6·5, 5·3, 1·5 and 0·27 times the initial piston radius respectively at the last cycle (i.e. $n = 150, 280, 60, 100$) in each case. This shows that the effect of cylindrical and spherical geometry has been fully taken into account in the first three cases whereas in the fourth case the shock has not travelled sufficiently far to show full effect of spherical geometry. Therefore, we may compare the results of the case 4 at $n = 100$ with those of case 2 at $n = 90$. We find that though the piston velocity in case 2 is slightly greater than that in case 4, the shock is stronger in case 4.

Fig. 3 shows the relation between Eulerian and Lagrangian distances and we find that after 150 and 280 cycles the radii of the piston in cases 1 and 2 have increased to 2·2 and 3·4 times the initial radii respectively. Further, we find that at a fixed time the disturbance due to cylindrical piston traverses a longer distance than that due to the spherical piston, the initial radii of both the cylindrical and spherical pistons being the same.

ACKNOWLEDGEMENT

The authors wish to express their gratitude to Prof. P. L. Bhatnagar for suggesting the problem and giving help and guidance throughout the preparation of this paper.

REFERENCES

1. TAYLOR, G. I., *Proc. Royal Soc.*, London, A 186 (1946), 273.

2. LIGHTHILL, M. J., *Quart. J. Mech. Appl. Maths.*, 1 (1948), 309.

3. VON NEUMANN, J. & RICHTMYER, R. D., *J. Appl. Phys.*, 21 (1950), 232.

4. COURANT, R. & FRIEDRICHS, K. O., "Supersonic Flow and Shock Waves" (Interscience Publishers Inc. New York), 1948, p. 8.

5. BHATNAGAR, P. L., SACHDEV, P. L. & PRASAD, P., "Spherical Piston Problem in Water" *J. Fluid Mech.* (Under Print).

6. RICHTMYER, R. D., "Difference Methods for Initial Value Problems" (Wiley Interscience, New York), 1967, p. 306.